Chemical Engineering Journal 101 (2004) 347–356

Chemical Engineering Journal

www.elsevier.com/locate/cej

Numerical simulation of temperature distribution inside microfabricated free flow electrophoresis module

Hideyuki Matsumoto [a,*], Nobuaki Komatsubara [a], Chiaki Kuroda [a], Nobuyoshi Tajima [b], Etsuo Shinohara [b], Hirobumi Suzuki [b]

[a] *Department of Chemical Engineering, Tokyo Institute of Technology, 2-12-1 Ookayama, Meguro-ku, Tokyo 152-8550, Japan*
[b] *Genome Medical Business Division, Olympus Optical Co. Ltd., 2-3 Kuboyama-cho, Hachioji-shi, Tokyo 192-8512, Japan*

Received 31 July 2003; accepted 28 October 2003

Abstract

Recently, Olympus Optical Co. Ltd. has developed a miniaturized device of two-dimensional free flow electrophoresis, and announces it as "microfabricated free flow electrophoresis (mFFE) module". It is significant for efficient design of the module to do numerical simulation of the dynamic behavior in the mFFE process. Thus, we try to do numerical simulation of temperature distribution inside a chamber of the mFFE module, based on the concept of the hybrid model simulation. As to the electroosmotic flow, it is proposed that output of Helmholtz–Smoluchowski equation model updates dynamically the boundary condition (the *x*-direction velocity of the walls) of the pressure driven flow model by introducing "user-defined functions" in the Fluent 6.0. As results of this hybrid model simulation by using the commercial code, it is confirmed that the simulation method can estimate heterogeneous distributions of temperature inside the mFFE module, which are seen in experimental results. Hence, it is considered that the simulation method is simple and practical for the basic design of the mFFE module. And it is necessary for the detailed design of the module to introduce the models, which are relevant to materials and geometrical structure of the module, into the hybrid model simulation system.

Keywords: Computational fluid dynamics; Miniaturized module; Free flow electrophoresis; Electroosmotic flow; Hybrid model simulation

1. Introduction

Free flow electrophoresis is well known as an analytical and a preparative method [1]. Scale-up of the free flow electrophoresis device is generally considered to be uneasy, because it needs supply of very high voltage and generates a large amount of joule heat that is not removed easily. On the other hand, miniaturization of the device [2] is said to be useful for analysis of a small amount of sample, and it is considered to have the merit of removing easily generated heat.

Recently, Olympus Optical Co. Ltd. has developed a miniaturized device of two-dimensional free flow electrophoresis, and announces it as "microfabricated free flow electrophoresis (mFFE) module" [3]. An mFFE module is manufactured by using photolithography and wet etching, which has a slit of high aspect ratio (e.g. 1:1:0.0006) between two Pyrex glass plates. It is considered that the mFFE module is applicable to separation of protein or DNA in the stage of preparation.

In research and development of the miniaturized module, there is a problem of large cost in the trial manufacture, which is done by considering three-dimensional transport phenomena inside the module. Therefore, in the industrial field, it is significant for efficient design of the module to carry out numerical simulation of the dynamic behavior in the micro chemical process such as the mFFE process. In the numerical simulation for designing micro chemical process, it is important to choose an appropriate modeling method by considering characteristic process behavior in the space of micrometer scale. On the other hand, only macroscopic models of the characteristic process behavior may be sufficient from the viewpoint of practical process design. For example when spatial heterogeneity of process variables inside the micro channel is found to affect dynamic behavior of the overall process remarkably, the important problem is what model should be chosen in the process dynamic simulation. Generally, a process designer applies only partial differential equation model to the accurate simulation. However, there is a case that the application of the model increases a load of the simulation to the designer. In the case, we would like to propose a simulation method that combines

* Corresponding author. Tel.: +81-3-5734-2140; fax: +81-3-5734-2140.
E-mail address: hmatsumo@chemeng.titech.ac.jp (H. Matsumoto).

1385-8947/$ – see front matter © 2004 Elsevier B.V. All rights reserved.
doi:10.1016/j.cej.2003.10.024

Nomenclature

C_{i0}	concentration of species i ($kg\,m^{-3}$)
C_p	specific heat capacity ($J\,kg^{-1}\,K^{-1}$)
d_c	depth of chamber (μm)
E	potential gradient ($V\,m^{-1}$)
I	current (A)
L_D	Debye length (m)
n_i	charge number of species i (–)
q	quantum of electricity (C)
T	temperature (K)
U	velocity ($m\,s^{-1}$)
V	supplied voltage (V)
w_c	width of the chamber (mm)
ε	dielectric constant ($F\,m^{-1}$)
ϕ	electric potential (V)
η	viscosity (Pa s)
ρ	density ($kg\,m^{-3}$)
κ	Boltzmann constant ($J\,K^{-1}$)
σ_w	charge density in the compact double layer ($C\,m^{-2}$)
ς	zeta potential (V)

dynamically the partial differential equation model with the other macroscopic models, which are a regression model, a neural network model, an algebraic equation model, and an ordinary differential equation model. And we call such the method "hybrid model simulation method" [4]. In the hybrid model simulation system, process information should be exchanged more effectively among the different models, which could make it possible to decrease loads to process designers in dynamic simulation for unsteady operation.

As to the mFFE module, it is observed by thermography that a large hot spot occurs near the platinum anode and spreads in operating the module, especially when supplied voltage is high. This is an important problem because such a high temperature may change characteristics of proteins and DNA. As factors relating to the heterogeneous distribution of temperature, we assume the joule heat generation, the pressure driven flow, the electroosmotic flow and so on. Thus, computational fluid dynamics (CFD) simulation [5] is considered to be useful in designing the mFFE process. However, for the CFD simulation by using commercial CFD softwares, it is necessary how to select appropriate numerical models that can estimate the electroosmotic flow, which is one of the characteristic phenomena in micro channels [6]. It is important for an efficient design of the process to investigate how to code the electroosmotic flow model in the commercial CFD software by considering both load and accuracy of simulation.

In this study, we try to do numerical simulation of temperature distribution, which is influenced by the electroosmotic flow, inside a chamber of the mFFE module by using the commercial CFD software "Fluent 6.0". Purposes of this study are to propose an efficient CFD simulation method using a commercial code, which is based on the concept of the hybrid model simulation, for the mFFE process, and to investigate applicability of the simulation method to designing the mFFE module from the viewpoint of practical use.

2. Principle of mFFE, process modeling and simulation system

2.1. Microfabricated free flow electrophoresis (mFFE)

As shown in Fig. 1, the size of mFFE module is ϕ 100 mm × 2 mm. Inside the module developed by means of microfabrication technology, there is a chamber for electrophoresis, size of which is 56.5 mm × 35 mm × 30 μm [3]. Namely, the shape of the chamber is so shallow in depth compare to the width, and its aspect ratio is about 1:1000. Seven inlets of carrier buffers, three inlets of sample and 21 outlets are formed on the module. Then, two electrodes are set on the both edges parallel to the direction of carrier flow.

In operating the mFFE process, it is considered that the carrier flow in the chamber shows very stable laminar flow. The sample solution is injected continuously as a narrow band into the carrier flow. An electric field is applied perpendicular to the carrier flow, so that sample components are separated laterally according to differences in electrophoretic mobility. Moreover, it is said that electroosmotic flow occurs from anode to cathode, which influences the degree of sample component's migration. The separated components are collected continuously at the outlets.

Then, some problems are found in operation of this mFFE process. For example stagnation of flow is easily caused in regions near the inlets and outlets. Also, temperature inside the module increases, which easily causes generation of air bubbles. Fig. 2 shows a result of temperature distributions of module's upper surface, which are measured by thermography, in the case when 20 mM Gly–Tris buffer, which of pH is 8.0, and 10% EtOH are used as the carrier solutions. At the time when 3 min elapse from start of supplying high voltage of 7 kV, large hot spot is seen in the region near the anode (right side in Fig. 2). Then, it is considered by the experimental results that the temperature distributions are influenced by the joule heat generation, the pressure driven flow, the electroosmotic flow and so on. Namely, in process simulation for designing the mFFE module, it is necessary to consider influence of the electroosmotic flow to dynamic behavior of the overall process.

2.2. Modeling of electroosmotic flow

Electroosmotic flow is characteristic phenomena in many applications of microsystems [7] like Lab-On-Chip or micro reactors and in micro process engineering. Therefore, many researchers [8–11] have reported modeling methods of the electroosmotic flow. In this subsection, models of the electroosmotic flow are derived by considering microscopic behaviors of ions near walls.

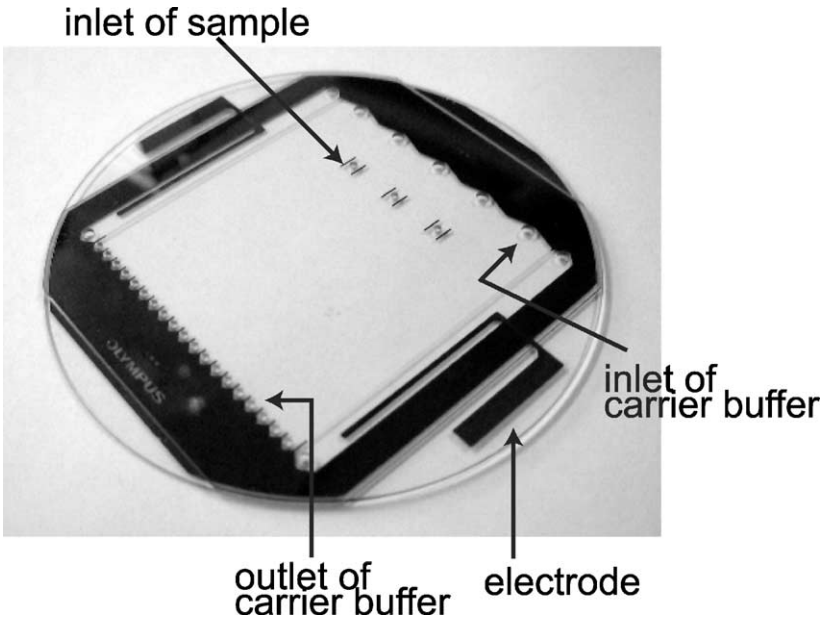

Fig. 1. Schematic layout of a mFFE module.

When wall of channel is made of glass, minus ions are charged on the wall. Then, plus ions congregate near the wall, and the compact double layer and the diffusive layer are formed so that thermal motions of ions perturb Coulomb force between the ions. The distribution of electric potential $\hat{\phi}(= \phi - \phi_0)$ can be written in Poisson–Boltzmann equation.

$$\nabla^2\hat{\phi} = -\frac{1}{\varepsilon}\sum_i n_i q C_{i0} \exp\left(-\frac{n_i q\hat{\phi}}{kT}\right) \quad (1)$$

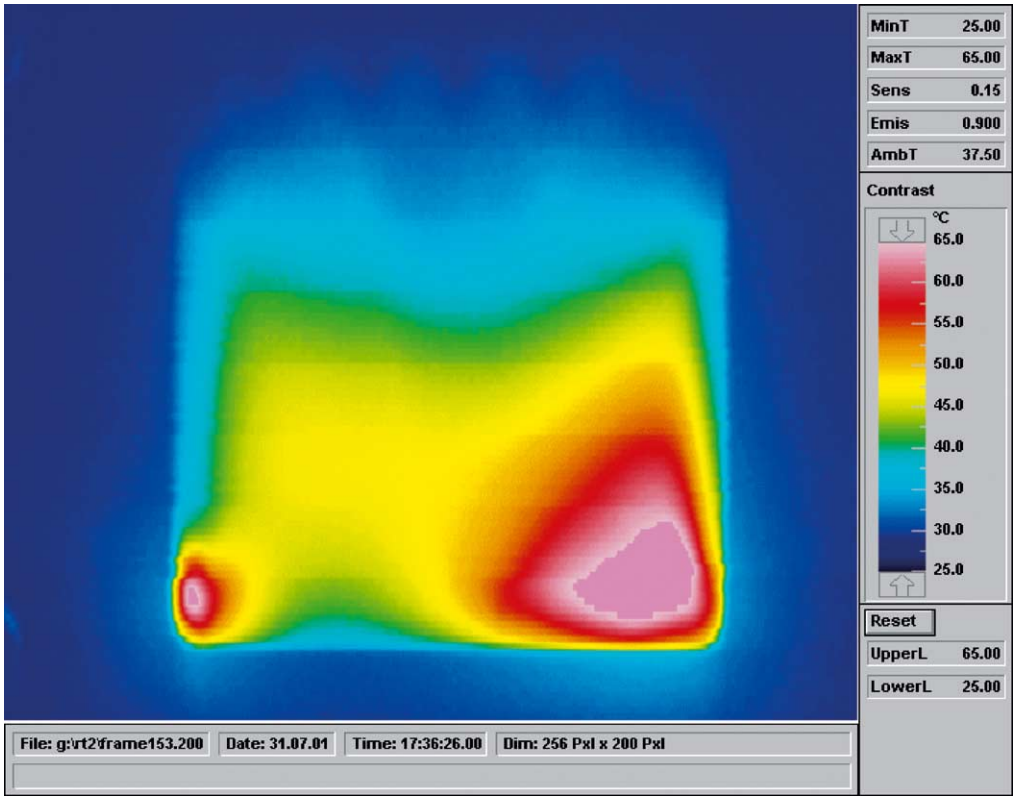

Fig. 2. An experimental result of temperature distributions on the mFFE module (buffer: 20 mM Gly–Tris pH 8.0 + 10% EtOH, $V = 0.7$ kV, $I = 0.75$ mA, $t = 3$ min).

By using Debye–Hückel approximation [6], Eq. (1) is rewritten as follows:

$$\nabla^2\hat{\phi} \approx -\frac{1}{\varepsilon}\sum_i n_i q C_{i0} + \frac{q^2}{\varepsilon kT}\left(\sum_i n_i^2 C_{i0}\right)\hat{\phi} \tag{2}$$

For equilibrium neutrality of charge, value of the first term in right side of Eq. (2) is close to zero. Hence, Eq. (3) is derived from Eq. (2) using the charge screening length L_D, which is so-called "Debye length".

$$\phi(y) = \phi_0 \exp\left(\frac{-z}{L_D}\right) \tag{3}$$

$$L_D = \left(\frac{q^2}{\varepsilon kT}\sum_i n_i^2 C_{i0}\right)^{-1/2} \tag{4}$$

Namely, distribution of potential has a characteristic exponential dependence with a decay length of L_D or the potential distribution is roughly screened out in $3L_D$.

Then, on the assumption that L_D is much smaller than the channel diameter, models of the electroosmotic flow are derived as follows. In steady state, when there is no pressure gradient in the channel and the flow is laminar, Eq. (5) is derived from the Navier–Stokes equation.

$$\eta\nabla^2 U + \rho_e E = 0 \tag{5}$$

As show in Fig. 3, it is assumed that the electric field E can only affect the charges in the diffusive layer with non-slip boundary conditions, and that the velocity U_x is a function of only z. Therefore, Eq. (5) is rewritten to Eq. (7), using Eq. (6).

$$\rho_e = -\frac{\sigma_w}{L_D}\exp\left(-\frac{z}{L_D}\right) \tag{6}$$

where σ_w is the charge density in the compact double layer.

$$\frac{d^2U_x}{dz^2} = -\frac{\sigma_w E}{\eta L_D}\exp\left(-\frac{z}{L_D}\right) \tag{7}$$

Hence, velocity distribution from the bottom wall is derived by the above-mentioned boundary condition ($U_x = 0$ at the wall).

$$U_x \cong \frac{\sigma_w E L_D}{\eta}\left[1 - \exp\left(-\frac{z}{L_D}\right)\right] \tag{8}$$

2.3. Hybrid model simulation system

In the previous work [4], we applied the hybrid model simulation method to dynamic simulation of polymerization process. In the dynamic simulation, ordinary differential equation (ODE) models, which many process designers are familiar with, are applied to the simulation of the overall region inside a reactor. On the other hand, partial differential equation (PDE) models are also applied to simulation for a region inside the reactor where spatial heterogeneity of state variables is remarkable, by considering whether the spatial heterogeneity affects dynamic behavior of the whole process. In the implementation of the dynamic simulation, process data are dynamically exchanged between ODE and PDE model in order to estimate dynamic behavior of the overall polymerization process.

Namely, it is the hybrid model simulation that each of the different models is applied to an appropriate region, in order to satisfy both problems of lightening a load of simulation and of simulating more accurately dynamic process behavior in a chemical device. Then, in order to carry out the hybrid model simulation of the whole process accurately and efficiently, it is important to make an interface module through which different solvers can work cooperatively. Fig. 4 shows a framework of the hybrid model simulation system, which consists of two solvers of ODE and PDE models. In the simulation system, two steps of calculation are iterated. At the first step, both solvers of the ODE and the PDE models are implemented simultaneously for estimating process behaviors during the simulation increment time Δt_i. Then, at the next, process data at the time $t + \Delta t_i$ are exchanged between two solvers through interface modules that can synchronize

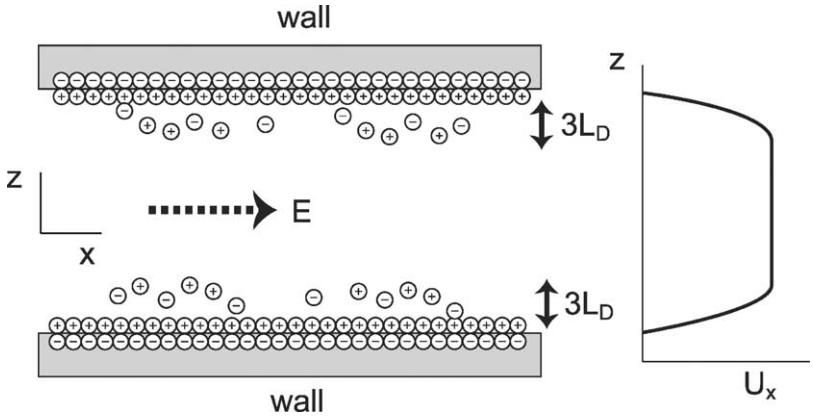

Fig. 3. Microscopic mechanism and velocity profile of electroosmotic flow.

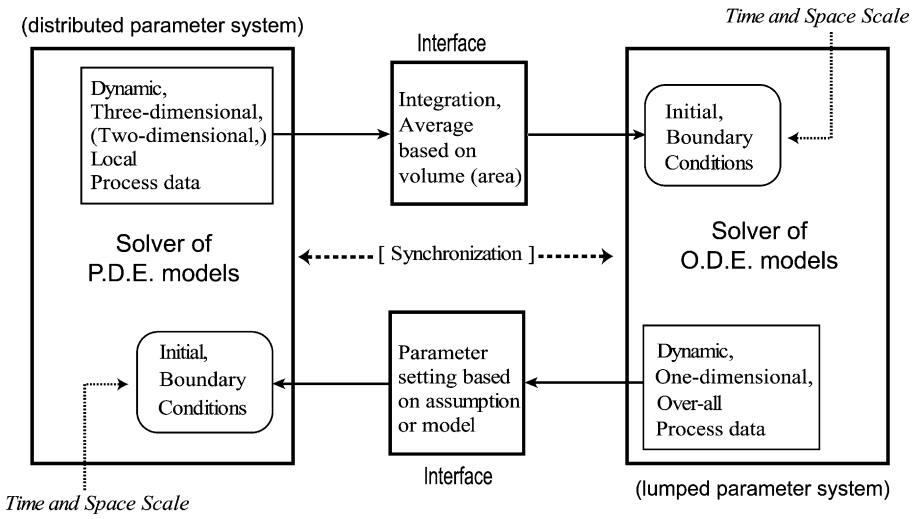

Fig. 4. Framework of a hybrid model simulation system.

with the solvers by communication. And implementations of two solvers are restarted after exchanging of the data. For example as shown in Fig. 4, the interface module takes an average of numerical data calculated by the solver of PDE models, and sends the average data of the region, which ODE models is applied to, to another solver. At the same time, another interface sends numerical data of the region, which ODE models is applied to, to the solver of PDE models as resetting boundary conditions.

As to CFD simulation of the mFFE process in this study, it is the important problem how to combine models of the electroosmotic flow with models of the pressure driven flow of carrier, based on the above-mentioned concept of the hybrid model simulation system. For example the Navier–Stokes equation model is used for simulating the pressure driven flow. Then, in the commercial CFD software, it is necessary for the efficient and accurate design how to select either microscopic or macroscopic model of the electroosmotic flow, which flows perpendicular to the pressure driven flow. Moreover, it is significant to make interface modules using a commercial code, so that the selected model of electroosmotic flow is dynamically combined with the Navier–Stokes equation model. It is considered that the interface modules made by a commercial code, which are based on the above-mentioned concept of the hybrid simulation, brings about a practical and efficient simulation for designing the mFFE process.

3. Results and discussions

3.1. CFD simulation method for designing mFFE process

In this study, we tried to do numerical simulation of three-dimensional temperature distribution inside a chamber of the mFFE module, by considering models of the electroosmotic flow. A CFD pre-processor “GAMBIT 2.0” and a CFD solver “Fluent 6.0”, which were developed by Fluent Inc., were used in this simulation. As shown in Fig. 5(a) and (b), an analytical region of a chamber in the mFFE module consists of three parts of space, by referring to the module made by Olympus Optical Co. Ltd. First, the space for electrophoresis and the space for electrodes have 50 μm in depth. The connection space between the

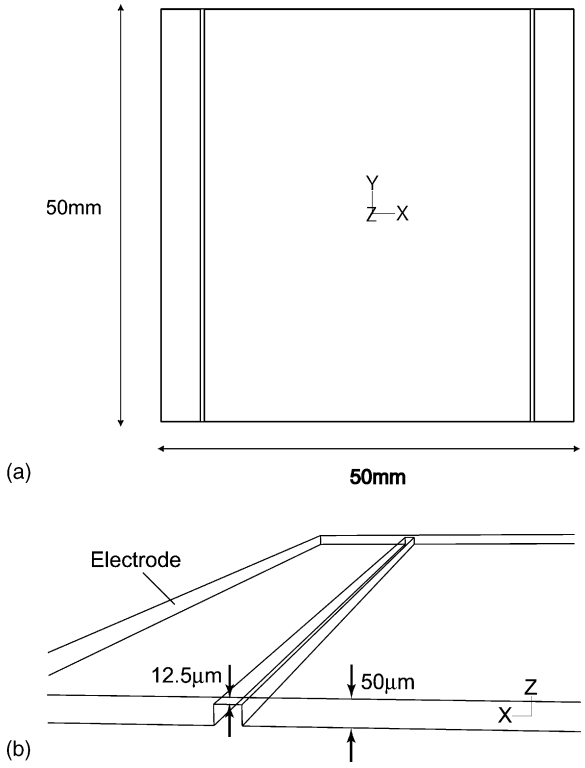

Fig. 5. Computational domain: (a) a view from the upper side of the chamber; (b) a view from the lateral of the chamber.

above-mentioned two spaces has a gap of 12.5 μm to inhibit from entering of bubbles generated on electrode to the space for electrophoresis. Then, the size of horizontal plane of the total regions is 50 mm × 50 mm, and so the analytical region has the shape of high aspect ratio. Thus, the analytical region was divided into about 31,500 square meshes of high aspect ratio by considering decrease of a load of simulation.

In the simulation, it was set that the carrier buffer flowed by pressure force into the rear face in Fig. 5(b), and that it flowed out from the front face. And it was assumed that the electrodes were set on the side faces of the analytical region. Geometrical structure of the chamber is simple compared with the actual module that is described in the previous section, so that the simulation can analyze relationship between the pressure driven flow model and the electroosmotic flow model without considering influences of flow's stagnation near inlets and outlets to the process behavior. In modeling the pressure driven flow of carrier, Navier–Stokes equation was used because the mFFE module was operated under low Reynolds number conditions. Moreover, energy equation model was also used and solved simultaneously.

As explained in Section 2.2, the electroosmotic flow is caused by migrations of ions in regions near walls. On some assumptions of one-dimensional flow and no pressure gradient in the chamber, a model of the electroosmotic flow can be written in Eq. (5). Then, as one of simulation methods, it is considered that this second-order differential equation is solved with above-mentioned Navier–Stokes equation and energy equation. In the preprocessing for the CFD simulation, it is necessary to divide the analytical region near the walls into many meshes of nanometer scale when the Debye length L_D is much smaller than chamber's depth of micrometer scale. For example in the case of 1 M KCl, L_D is about 0.3 nm, which needs very small meshes and increases a load of simulation. Thus, when the depth of the chamber is much larger than the length of L_D, it can be assumed that the electroosmotic flow is the plug flow. The plug flow model is derived from Eq. (8).

$$U_{eof} = \frac{\sigma_w E L_D}{\eta} \tag{9}$$

By using $L_D = \varsigma\varepsilon/\sigma_w$, Eq. (9) can be written to Eq. (10), which is so-called "Helmholtz–Smoluchowski equation" [12].

$$U_{eof} = \frac{\varepsilon\varsigma E}{\eta_{eof}} \tag{10}$$

Hence, we would like to propose a simulation method that the value of U_{eof}, which was calculated by Eq. (10), was set to velocity of the top and bottom walls as boundary conditions of the pressure driven flow model. That was to combine macroscopic model of the plug flow in only the x-direction with the Navier–Stokes equation model. Then, it was assumed that amount of increase of temperature on the electrodes changed with the supplied voltage V and the current I as follows:

$$\Delta T = \frac{IV}{w_c^2 d_c \rho C_p} \tag{11}$$

Moreover, it was set that viscosity η in a local region changed with the temperature T.

$$\eta = a \exp\left(\frac{1 + bT}{cT + dT^2}\right) \tag{12}$$

where the values of a, b, c, and d was 1.26×10^{-2}, -5.81×10^{-3}, 1.13×10^{-3}, and -5.72×10^{-6}. However, in this study, it was assumed that the value of U_{eof} was estimated from the constant value of viscosity η_{eof}.

Hence, in this dynamic simulation, we tried to combine these algebraic equation models, which were the model of electroosmotic flow (Eq. (10)), the model of rise of temperature (Eq. (11)) and the model of viscosity's change (Eq. (12)), with the partial differential equation models of momentum and heat transport phenomena. Then, the interface modules among these models were coded by using "user-defined functions" (UDF) in the Fluent 6.0. The UDF made it possible to update dynamically the initial conditions and boundary conditions in the partial differential equation models by outputs of above-mentioned algebraic equation models. As to the electroosmotic flow, it could be said that the model and its interface module were easily coded in the Fluent 6.0, by using the classical model of "Helmholtz–Smoluchowski equation". Namely, it was considered that this hybrid model simulation became simple and applicable for the basic design of the mFFE module, by introducing some assumptions corresponding to the transport phenomena and by modeling these assumptions using the commercial code.

Table 1
Physical properties in the simulation

ρ (kg m^{-3})	1.0×10^3
η_{eof} (Pa s)	1.0×10^{-3}
ε (F m^{-1})	7.805×10^{-10}
ς (V)	2.0×10^{-2}
C_p (J kg^{-1} K^{-1})	4.17×10^3

3.2. Implementation of hybrid model simulation

We carried out the simulation of the case when voltage V was 7 kV and current I was 0.75 mA, by using the values of physical properties shown in Table 1. Velocity of inlet flow was 1 mm s^{-1} and temperature of carrier was 298 K. As a result of the simulation, Fig. 6 shows temperature distribution of the face $z = 0$. The left side in Fig. 6 was the anode area, and so it was found that the distribution of high temperature spread from the anode area to the cathode area. Moreover, as shown in Fig. 7(a), higher velocities of the carrier flow were seen in the downstream region near the cathode, whereas the velocities near the anode were low. A

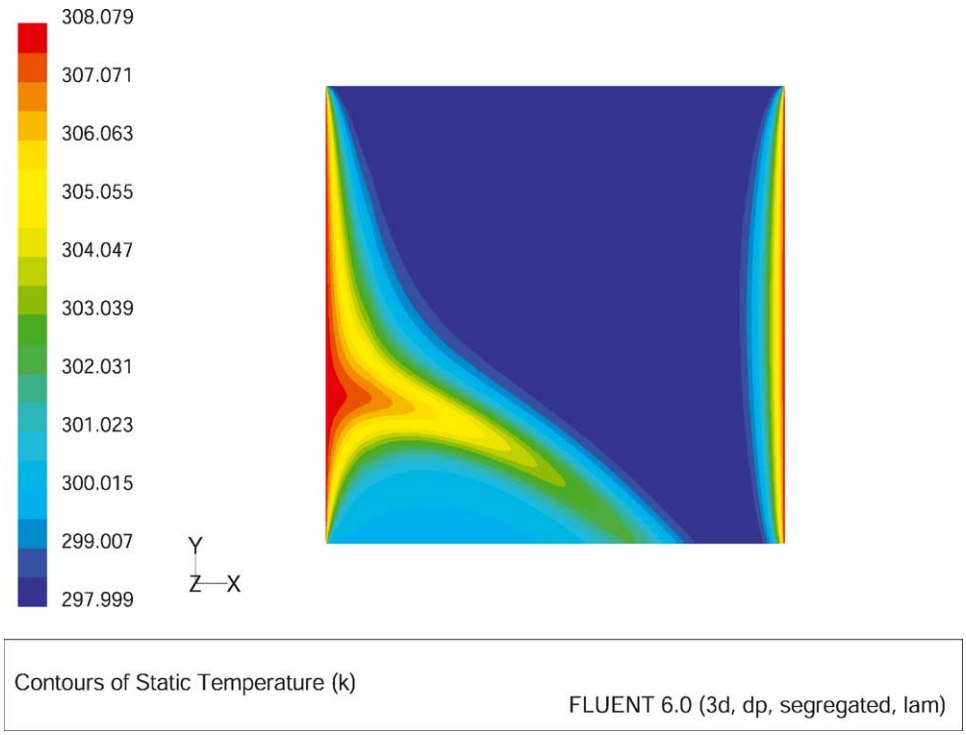

Fig. 6. Spatial distribution of temperature inside the chamber ($d_c = 50\,\mu m$, $V = 7\,kV$, $I = 0.75\,mA$, $z = 0$).

spot like stagnation was also seen near the anode. Therefore, it was considered that the electroosmotic flow hindered fluid of raised temperature near the anode from flowing out from the chamber rapidly, and that the dynamic behavior brought about distribution of high temperature in the regions near the anode. And, it was supposed that the spatial heterogeneity of velocity distributions non-linearly influenced broadening of concentration bands of the injected sample in the mFFE separation [13]. Moreover, when the velocity distribution of the face $z = +25\,\mu m$, as shown in Fig. 7(b), was compared with Fig. 7(a), it could be confirmed that the overall flows near the walls were slower than flows at the center of the slit. It was estimated that the velocity distributions in the direction were mainly caused by the pressure driven flow, because the one-dimensional Helmholtz–Smoluchowski equation model was used. If a differential equation for pressure change in the direction inside the electrical double layer [11] was introduced to the simulation, it would be estimated more accurately that the electroosmotic flow, which flowed perpendicular to the pressure driven flow, influenced three-dimensional heterogeneities of flow pattern inside the chamber.

Then, in this study, influence of the depth d_c of the chamber to temperature distribution was investigated. Fig. 8(a) shows temperature distribution of the face $z = 0$ in the case when voltage V is 3 kV and current I is 2.4 mA. And, Fig. 8(b) shows temperature distribution in the case when the depth is 500 μm, which is resulted from the same operational condition as the case of 50 μm (Fig. 8(a)). In Fig. 8(a), because regions of the high temperature were smaller as compared to Fig. 6, it was confirmed that influence of the electroosmotic flow to the pressure driven flow became weak by decreasing the value of the potential gradient E. Moreover, by comparing Fig. 8(a) with Fig. 8(b), it was recognized that temperature on the electrode increased with decrease of depth of the chamber and that the distributions of the higher temperature were broaden by the electroosmotic flow.

On the whole, the above-mentioned numerical simulations could estimate heterogeneous distributions of temperature inside the mFFE module, which were seen in experimental results (Fig. 2). In comparing the simulation data with the experimental data, it was supposed that the patterns of temperature distribution were changed by geometrical structure in the part of outlets [13]. Then, it was made clear that the electroosmotic flow was an important factor relating to heterogeneous distributions of temperature in designing the mFFE module. Moreover, it was significant to introduce the assumption of adiabatic walls to implementing the simulations. It was because the homogeneous distribution of temperature was estimated in the case when wall's temperature was equal to the outside temperature. Namely, it was considered that low thermal conductivity of Pyrex glass, which was used in the actual module, also influenced the spatial heterogeneity of temperature. Though it was generally known that micro channels showed good performance of heat exchange, there was found the important problem that new boundary conditions concerned with heat transfer should be introduced by considering materials of the walls.

Hence, it was found that this hybrid model simulation was applicable to the basic design of the mFFE process, from the viewpoint of practical use. Namely, results of this hybrid

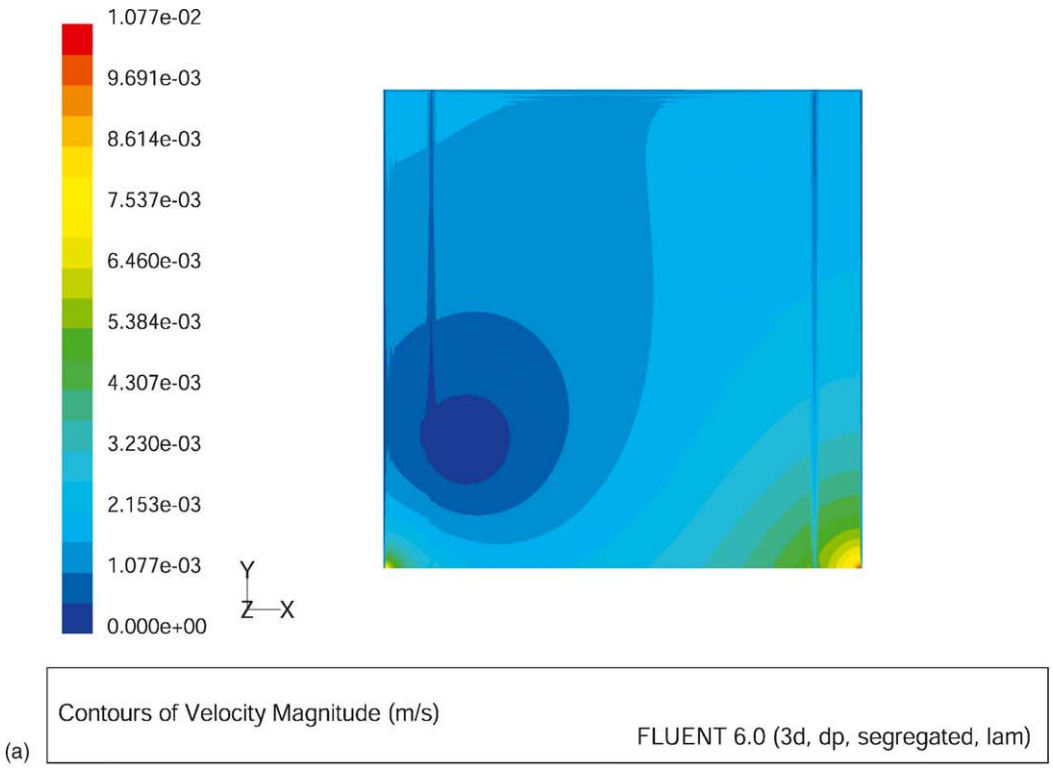

(a)

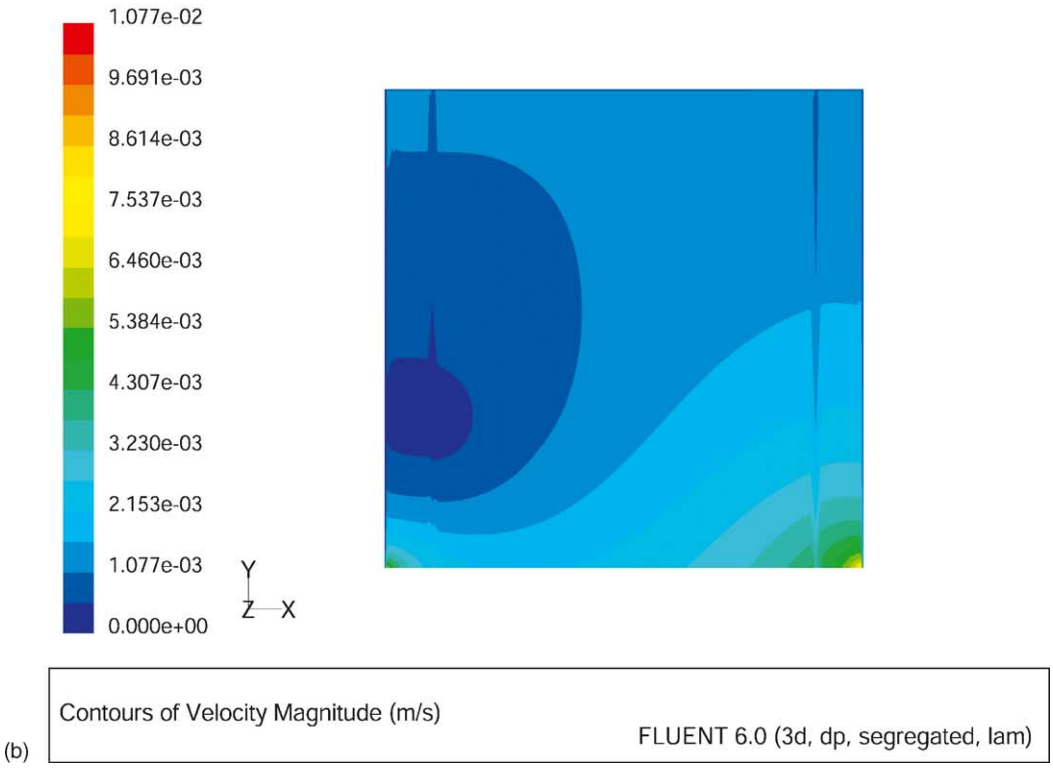

(b)

Fig. 7. Spatial distribution of velocity inside the chamber: (a) $d_c = 50\,\mu m$, $V = 7\,kV$, $I = 0.75\,mA$, $z = 0$; (b) $d_c = 50\,\mu m$, $V = 7\,kV$, $I = 0.75\,mA$, $z = +25\,\mu m$.

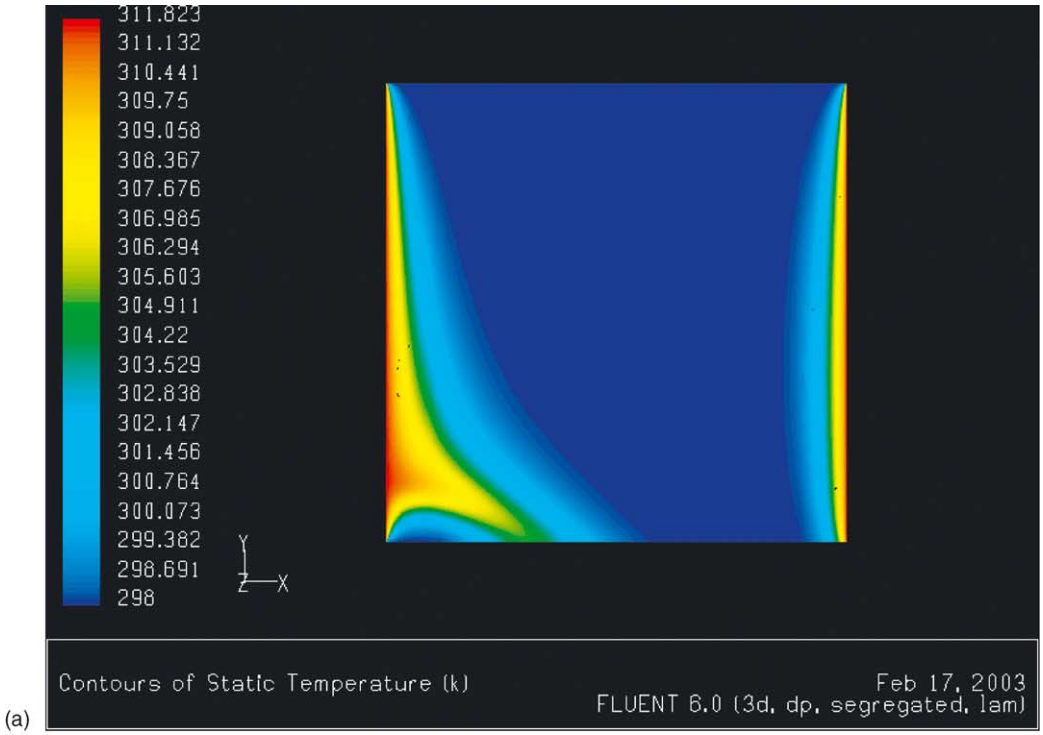

(a)

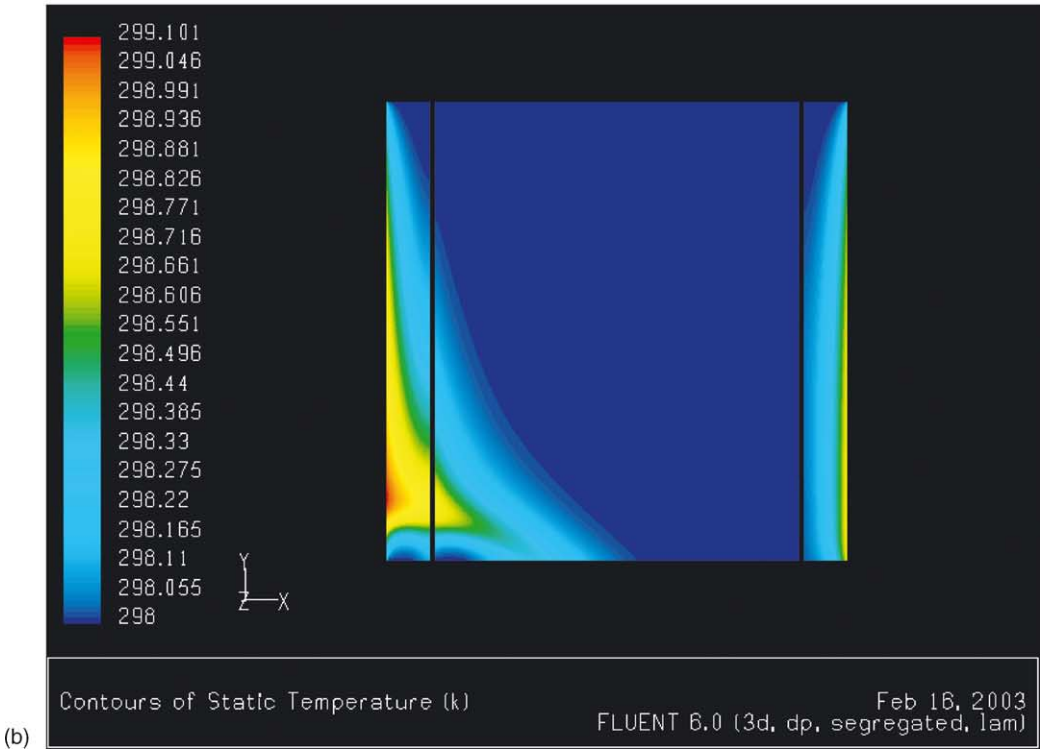

(b)

Fig. 8. Spatial distribution of temperature inside the chamber: (a) $d_c = 50\,\mu m$, $V = 3\,kV$, $I = 2.4\,mA$, $z = 0$; (b) $d_c = 500\,\mu m$, $V = 3\,kV$, $I = 2.4\,mA$, $z = 0$.

model simulation using the Helmholtz–Smoluchowski equation model could tell us whether dynamic simulations for the case that the length of double layer could not be neglected were in the ballpark or not. On the other hand, for the detailed design of the mFFE process, it was necessary to introduce the models, which were relevant to materials and geometrical structure of the module, into the dynamic simulation by using a commercial code. As to the electroosmotic flow, it was significant to consider spatial distributions of concentration and charge of solution, which could change local velocity of the electroosmotic flow dynamically in the simulation.

4. Conclusions

We tried to do numerical simulation of temperature distribution inside a chamber of the mFFE module, by considering models of electroosmotic flow. In the CFD simulation by using a commercial code, it was proposed how macroscopic models, which were the models of electroosmotic flow, of heat generation and of viscosity's change, were combined with the Navier–Stokes equation model and energy equation model, based on the concept of the hybrid model simulation. As to the electroosmotic flow, it was proposed that output of Helmholtz–Smoluchowski equation model updated the boundary condition (the *x*-direction velocity of the walls) of the pressure driven flow model by introducing "user-defined functions" in the Fluent 6.0.

As results of this hybrid model simulation, it was confirmed that the simulation method could estimate heterogeneous distributions of temperature inside the mFFE module, which were seen in experimental results. Thus, it was considered that the simulation method was simple and practical for the basic design of the mFFE module. Furthermore, it was necessary for detailed design of the module to introduce the models, which were relevant to materials and geometrical structure of the module, into the hybrid model simulation system. Then, it was the promising topic that optimal design of separation process in the mFFE module was made possible by introducing dynamic models for species transport to the hybrid model simulation system.

Acknowledgements

This work was partially supported by the Research Association of Micro Chemical Process Technology (MCPT) and the 21st Century COE Program (Chemical Field) of Tokyo Institute of Technology.

References

[1] L. Krivánková, P. Bocek, Continuous free-flow electrophoresis, Electrophoresis 19 (1998) 1064–1074.
[2] D.E. Raymond, A. Manz, H.M. Widmer, Continuous sample pretreatment using a free-flow electrophoresis device integrated onto a silicon chip, Anal. Chem. 66 (1994) 2858–2865.
[3] N. Tajima, J. Funazaki, H. Suzuki, E. Shinohara, A new application by microfabricated free flow electrophoresis module, in: Proceedings of the Micro TAS 2002, vol. 1, 2002, pp. 542–544.
[4] H. Matsumoto, C. Kuroda, Numerical simulation of dynamic behavior in a reactor using a hybrid model, Theor. Appl. Mech. Jpn. 51 (2002) 301–306.
[5] T.M. Grateful, E.N. Lightfoot Jr., Finite difference modeling of continuous-flow electrophoresis, J. Chromatogr. 594 (1992) 341–349.
[6] T. Ozawa, M. Sasaki, T. Yamaue, Simulator for micro flows, in: Proceedings of the 16th CFD Symposium, Tokyo, 2002, D310-1.
[7] J. Khandurina, A. Guttman, Bioanalysis in microfludic devices, J. Chromatogr. A 943 (2002) 159–183.
[8] D. Burgreen, F.R. Nakache, Electrokinetic flow in ultrafine capillary slits, J. Phys. Chem. 68 (1964) 1084–1091.
[9] C.L. Rice, R. Whitehead, Electrokinetic flow in a narrow cylindrical capillary, J. Phys. Chem. 69 (1965) 4017–4024.
[10] N.A. Patankar, H.H. Hu, Numerical simulation of electroosmotic flow, Anal. Chem. 70 (1998) 1870–1881.
[11] J.M. MacInns, Computation of reacting electrokinetic flow in microchannel geometries, Chem. Eng. Sci. 57 (2002) 4539–4558.
[12] B. Gaš, M. Štedrý, E. Kenndler, Contribution of the electroosmotic flow to peak broadening in capillary zone electrophoresis with uniform zeta potential, J. Chromatogr. A 709 (1995) 63–68.
[13] G. Weber, P. Bocek, Optimized continuous flow electrophoresis, Electrophoresis 17 (1996) 1906–1910.